

Dephasing times of the vibrons in α -N₂ and in α -(¹⁵N₂)_x(¹⁴N₂)_{1-x} mixed crystals

Jan De Kinder, Etienne Goovaerts, August Bouwen, and Dirk Schoemaker
Physics Department, University of Antwerp (UIA), B-2610 Wilrijk, Antwerp, Belgium
(Received 2 April 1990)

Picosecond time-resolved coherent anti-Stokes Raman measurements were performed on the vibrons in single crystals of α -N₂ and on mixed crystals of α -(¹⁵N₂)_x(¹⁴N₂)_{1-x} with $0 \leq x \leq 0.086$. The observed dephasing of the vibrons in pure α -N₂ crystals is faster than exponential, and this is well described by adding a Gaussian factor. The Gaussian decay component is assigned to inhomogeneous broadening and could be observed as a result of the high time resolution of our setup. This indicates that the approximations often employed in the case of weak disorder are not applicable in the short-time region of the decay. The exponential dephasing is ascribed to scattering from anharmonic librations and low-frequency phonons. The A_g - T_g factor group splitting and its temperature dependence were determined through analysis of the beating pattern on the spectra, with an accuracy up to 0.007 cm^{-1} . In the isotopically mixed crystals, it is shown that the ¹⁵N₂ molecules do not act as trapping center for the ¹⁴N₂ vibrons. The homogeneous dephasing time for the ¹⁵N₂ molecules is surprisingly short compared to the ¹⁴N₂ decay.

I. INTRODUCTION

Specific information on vibrational and rotational interactions within a solid can be gained from a careful study of its infrared and Raman transitions. High-resolution Raman studies have already been performed on a large number of systems. However, for linewidths of about $\frac{1}{100}$ of a wave number, the resolution of spontaneous Raman measurements is outweighed¹ by stimulated Raman techniques,² both in frequency and in time domain. Higher resolution and no tradeoff between sensitivity and resolution is attained by the use of either single mode or pulsed lasers. Due to the availability of ultrashort light pulses, a higher dynamic range of resolution can be reached in the time domain.

Nitrogen solidifies³ at 63 K and zero pressure into a hexagonal hcp structure (space group $P6_3/mmc$). At 35.6 K, a structural and orientational phase transition occurs from the β to the α phase. In this cubic fcc phase with space group³ $Pa\bar{3}$, the molecules become oriented. The intramolecular vibration ($\Omega_v = 2328 \text{ cm}^{-1}$) of the nitrogen molecules, which is well separated from the phonons and librations ($\Omega \leq 70 \text{ cm}^{-1}$), is shifted by but a few wave numbers from its gas-phase value. The four N₂ stretching vibrations for each unit cell combine in A_g and T_g Raman-active modes at $\mathbf{k} \approx 0$, which are separated by about 1 cm^{-1} . The internal vibrations on different sites couple to wavelike excitations, called vibrons. Due to small intermolecular interactions, these Frenkel excitons⁴ formed from molecular vibrations constitute a narrow band (width $W \simeq 1.2 \text{ cm}^{-1}$).

In this paper we study the decay of the vibrons in α -N₂ by time-resolved coherent anti-Stokes Raman scattering^{1,5} (TR-CARS). In this technique, a Raman

transition is resonantly excited by the stimulated Raman process. By monitoring the coherent anti-Stokes scattering of this excited population, the dephasing of the excited molecules is determined. The contributions to this dephasing are usually divided into population decay and pure dephasing processes. Since population decay of the N₂ vibration is known to proceed very slowly, e.g., $T_1 = 56 \text{ s}$ for the liquid,⁶ the observed decay is due to pure dephasing processes only. A dephasing time T_2 can be associated with the Raman transition, if the decay is exponential.

Klafter and Jortner⁷ developed a line-shape model for Frenkel excitons in molecular crystals with a Gaussian (mean-squared value σ) distribution of the site energies, assuming a weak exciton-phonon coupling. Two extreme situations may be discerned: (i) when $\sigma > W$, the band shape is determined by the inhomogeneous energy distribution; (ii) when $\sigma \ll W$, in general a line shape with a much narrower width compared to σ results, given by

$$I(\omega) = \frac{\pi \sigma^2 \rho(\omega)}{(\omega - \omega_0)^2 + [\pi \sigma^2 \rho(\omega)]^2} \quad (1)$$

with $\rho(\omega)$ the exciton density of states. For slowly varying $\rho(\omega)$, the line shape is Lorentzian to a good approximation. This is no longer valid near band singularities, such as for the $\mathbf{k} = 0$ state of the A_g vibron. An asymmetric line shape is then expected to result.⁸

The value of σ , the spread of site energies, cannot simply be obtained from the inhomogeneous line broadening of the vibrons in α -N₂, since this value may be affected by the vibron coupling. However, a substitutional impurity can act as a probe for the local disorder and σ is then determined by the inhomogeneous broadening of one of its optical transitions. Hereto, we performed mea-

measurements on crystals doped with the isotopic impurity $^{15}\text{N}_2$, which is an ideal substitute for the host molecule with but a small distortion of the lattice.

The relaxation of the A_g vibron was previously⁹ investigated on a ns time scale using time-resolved stimulated Raman scattering and was found to be nonexponential with an effective (exponential) decay time increasing with time. A calculated $\exp \sqrt{t/\tau}$ dependence^{7,8} was derived in the long-time limit for the decay of a coherent state in a molecular crystal with weak disorder ($\sigma \ll W$), and could be fitted to the experimental results yielding $\tau=17$ ns. Our results on a ps time scale cannot be analyzed even qualitatively within this framework. The high time resolution and sensitivity of our measurements were exploited to uncover both inhomogeneous and homogeneous contributions to the line broadening. Although σ (between 0.01 and 0.05 cm^{-1}) is smaller than W (1.2 cm^{-1}), it was still possible to observe small inhomogeneous contributions to the observed dephasing.

TR-CARS experiments were performed on pure $^{14}\text{N}_2$ crystals and on mixed crystals of $^{14}\text{N}_2$ with up to 8.6 mol% of $^{15}\text{N}_2$. Our preliminary results¹⁰ on $^{14}\text{N}_2$ crystals were extended and slightly corrected after recalibration of our apparatus. For mixed crystals of $^{14}\text{N}_2$ with $^{15}\text{N}_2$, both the dephasing of the $^{14}\text{N}_2$ vibrons and the $^{15}\text{N}_2$ stretching vibration were investigated. Inhomogeneous and homogeneous components were properly separated and beating patterns due to the factor group splitting of the A_g and the T_g mode were analyzed. Our results are also compared to very recent stimulated Raman gain (SRG) measurements¹¹ in the frequency domain performed on thin films (50–100 μm) of $\alpha\text{-N}_2$.

II. EXPERIMENTAL SETUP

Pulses from a mode-locked, pulse compressed Nd:YAG laser¹² were frequency doubled to produce 6-ps green pulses. One third of this beam was used to synchronously pump a R6G dye laser (pulse width: 600 fs). A second part was made collinear to the beam from the dye laser, in such a way that pulses from both beams were overlapping in time, thus forming the so-called pump pair. The wavelength of the dye laser was adjusted to 607 nm for resonant excitation of the internal vibration ($\Omega_v=2328$ cm^{-1}) of N_2 . The third part of the Nd:YAG laser (the probe beam) was led through an optical delay line and made collinear to the pump pair. The three beams were focused in the sample. Optimal phase matching for the TR-CARS signal was achieved by varying the distance between the two beams of the pump pair and the distance between the pump pair and the probe beam, thereby avoiding the phase-matching condition for the instantaneous CARS signals (generated by one pair of beams). The emergent radiation was first filtered using a cutoff filter; the anti-Stokes beam generated by the three beams was spatially separated from the still-present instantaneous CARS signal and focused onto the entrance slit of a double monochromator. Detection was performed by

means of a photomultiplier using single-photon counting. The decay of the excitation was recorded by varying the time delay of the probe pulse. The resolution of our setup was determined by recording the instantaneous CARS signal generated by the probe beam and the beam from the dye laser and was found to be 7 ps.

Measurements were performed on bulk crystals, which were carefully grown and slowly cooled through the α - β phase transition. $^{15}\text{N}_2$ isotopes were admixed in the gas phase: The concentration in the solid phase was determined by the relative strength of the spontaneous Raman scattering of the $^{15}\text{N}_2$ and $^{14}\text{N}_2$ molecules and was found to be equal to that in the gas phase. The distribution of the impurities throughout the sample was found to be homogeneous.

III. RESULTS

A. Pure $\alpha\text{-N}_2$ crystals

The TR-CARS decay (Fig. 1) observed for the vibrons in $\alpha\text{-N}_2$ is faster than exponential—the effective decay time increases with delay time—and shows a beating pattern. This pattern (with a period of about 33 ps) results from a coherent beating of the A_g and T_g vibron. Both these vibrons are excited because the spectral bandwidth of the dye laser—approximately 8 cm^{-1} —is larger than their energy splitting of about 1 cm^{-1} . A careful analysis of the beating pattern, which we performed both in time

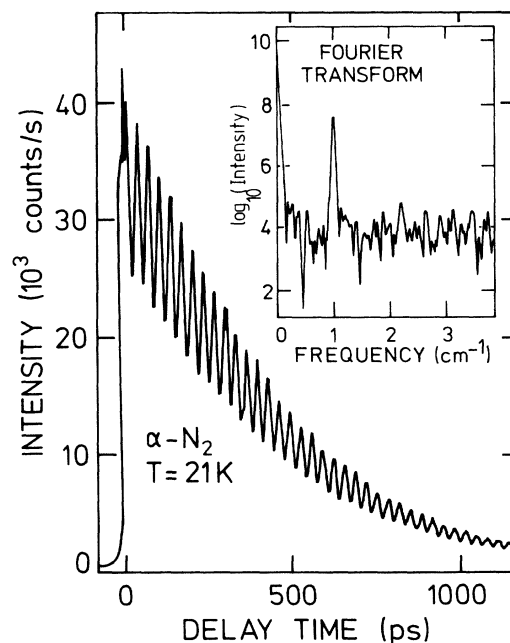


FIG. 1. Dephasing decay of the N_2 vibrons in $\alpha\text{-N}_2$ at 21 K and its Fourier transform (FT), shown in the inset. The beating pattern between the A_g and the T_g vibron in the time domain shows up in the FT spectrum as a sharp peak at about 1 cm^{-1} , about two orders of magnitude larger than the noise at neighboring frequencies.

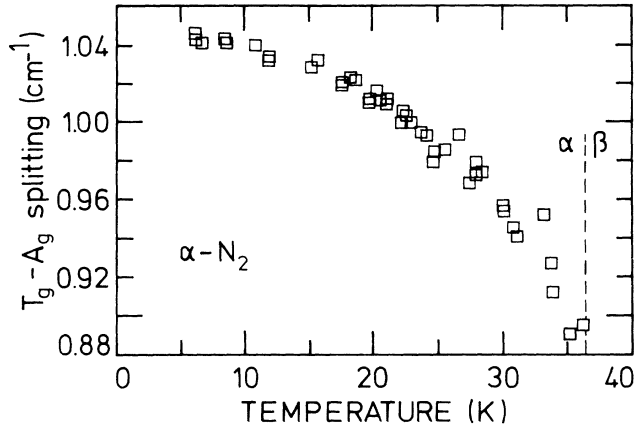


FIG. 2. Temperature dependence of the factor group splitting between the A_g and the T_g vibron. The energy difference decreases with increasing temperature towards the α - β phase transition temperature, also indicated in this figure.

(by fitting the obtained decay) and frequency space, after Fourier transforming the spectra (as in the inset of Fig. 1) allowed us to determine the A_g - T_g frequency splitting with an extremely high accuracy of 0.005 cm^{-1} at low temperature. At this temperature, the largest ratio of decay time to beating period is achieved. With increasing temperature, this ratio is reduced, thus enhancing the error on the determined factor group splitting. The Fourier transform method showed to be the most reliable one. The resulting factor group splitting as a function of temperature is plotted in Fig. 2. It decreases by about 16% between low temperature and the α - β phase transition at 36.5 K. At this temperature, the factor group splitting, which can be considered as an order parameter for the α - β phase transition, jumps to zero in a discontinuous way, as expected from the first-order character of this phase transition.

In contrast to the slower than exponential decay⁹ observed on the ns time scale, a faster than exponential decay is recorded on the ps time scale. We added a Gaussian decay factor to the fitted function to account for this faster decay, resulting in the following global functional behavior:

$$S(t) = (A_{A_g}^2 + A_{T_g}^2 + A_{A_g} A_{T_g} \cos \Omega t) e^{-t/T_2 - \Delta^2 t^2/2}. \quad (2)$$

Note that in this formula the same temporal behavior (T_2 , Δ) has been assumed for both the A_g and the T_g vibron. This treatment corresponds to the traditional way of separating homogeneous and inhomogeneous broadening,^{13,14} paying no attention to the vibronic character of the studied vibration and to the band narrowing⁷ following from it. It corresponds to the early time range in which the approximations that are usually applied for the $\sigma \ll W$ are not valid and higher-order terms in the applied expansions are being explored. The Gaussian contribution [full width at half maximum

(FWHM)], typically $\Delta=0.0068 \text{ cm}^{-1}$, was seen to vary appreciably on the position in the crystal and the growth procedure. This is a first indication that the Gaussian factor in Eq. (2) corresponds indeed to an inhomogeneous line broadening. Other evidence for this assignment will be provided further on in this paper.

An accurate determination of the exponential dephasing time $T_2/2$ was possible only for measurements in which the inhomogeneous contribution to the dephasing was small. The resulting dephasing time $T_2/2$ increases appreciably for decreasing temperature, as is shown in Fig. 3. It is interesting to note that the measurements of Ref. 9 were performed with resolution of several ns, and could only reveal the long time tail of the decay. Evidently, neither the exponential nor the Gaussian decay factors determined in our experiments can be observed in that time region. Also, no temperature dependence was noticed.

The linewidth corresponding to the exponential decay times, $T_2/2$ in our TR-CARS experiments, is much smaller than the ones measured by a recent high-resolution SRG study.¹¹ At 21 K, we obtained a Lorentzian FWHM of 0.013 cm^{-1} , whereas in Ref. 11 global linewidths of 0.041 cm^{-1} for the A_g and 0.053 cm^{-1} for the T_g vibron were obtained. This may originate¹⁵ from a larger number of crystalline domains in their sampling volume, since a large focal spot size was necessary to avoid sample damage due to high laser power and the likely possibility that the thin-film sample consisted of smaller crystalline domains than our bulk single crystal. Very recently,¹⁶ smaller linewidths were found in bulk α -N₂ samples, close to the Lorentzian width derived from our decay times T_2 . This further supports the assignment of the Gaussian component as being due to inhomogeneous broadening processes.

The decay time increases from 113 to 168 ps (Ref. 10) when passing from the α to the β phase. This anomalous behavior is caused by the structural and orientational phase transition from a cubic (fcc) phase with static N₂

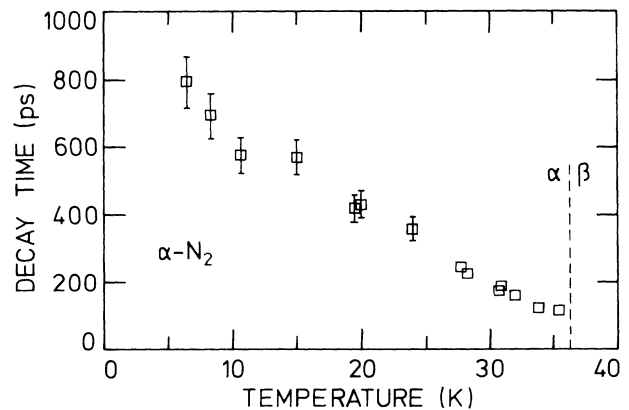


FIG. 3. The decay time, $T_2/2$, as a function of temperature in α -N₂. The α - β transition temperature is indicated by a dashed line. The experimental error on the decay times is about 10%.

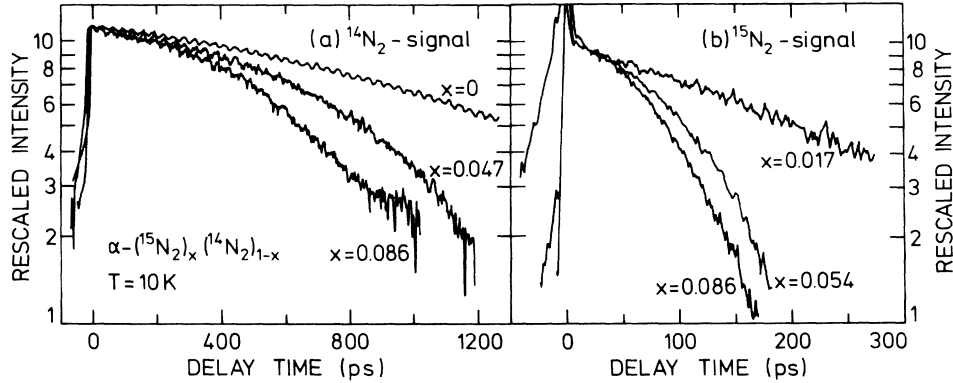


FIG. 4. Normalized decay spectra (a) for the $^{14}\text{N}_2$ vibrons and (b) for the $^{15}\text{N}_2$ stretching vibration, in isotopically mixed crystals $\alpha\text{-(}^{14}\text{N}_2)_x\text{(}^{15}\text{N}_2)_{1-x}$. The decay time of the isolated $^{15}\text{N}_2$ vibration is much smaller than that of the $^{14}\text{N}_2$ vibrons. The contribution of inhomogeneous broadening increases for increasing concentrations of $^{15}\text{N}_2$.

orientation to a hexagonal (hcp) one without ordering in the sublattices.

In the above analysis, the same dephasing constants (T_2 , Δ) were adopted for the A_g and the T_g vibron. Since the A_g vibron corresponds to a singularity of the density of states, the usual approximations leading to a Lorentzian line shape (i.e., exponential decay) are no longer valid.^{7,8} Hence a drastically different decay functional would be expected for the A_g and the T_g vibron. In order to investigate this effect, we generalized the fitting function (2) to include a separate decay time, $T_2(A_g)$ and $T_2(T_g)$ for both vibrons. The decay of the beating term, τ_{beat} is then related to these decay times by¹⁷

$$\frac{1}{\tau_{\text{beat}}} = \frac{1}{2} \left(\frac{1}{T_2(A_g)} + \frac{1}{T_2(T_g)} \right). \quad (3)$$

We carefully analyzed the decay of the beating amplitude and compared decay times for the full signal and the beating amplitude. However, we could not resolve a difference in the behavior between the decay of the whole spectra and the decay of the beating amplitude within experimental error. Beck and Nibler¹¹ found for the linewidth of the A_g vibron 0.010 cm^{-1} , and for the T_g vibron 0.016 cm^{-1} , both at 17 K. Such a small difference in linewidth could not be resolved from the direct fitting of our decay spectra, mainly because of the large number of fitting parameters.

B. Mixed $(^{14}\text{N}_2)_{1-x}(^{15}\text{N}_2)_x$ crystals

Mixed isotopic crystals with $^{15}\text{N}_2$ concentration up to 8.6 mol% were grown. For a small concentration (1.7 mol%) of $^{15}\text{N}_2$, an almost purely exponential dephasing of the $^{15}\text{N}_2$ vibration was found with a surprisingly short decay time $T_2/2=(160\pm 10)$ ps at 10 K, as shown in Fig. 4(b). This value corresponds to a linewidth, smaller by almost a factor of 2 than was obtained for the natural concentration of $^{14}\text{N}^{15}\text{N}$ in Ref. 11. It seems that the same linewidth should be observed for substitutional

$^{15}\text{N}_2$ and $^{14}\text{N}^{15}\text{N}$ molecules and, most probably, inhomogeneous broadening of their spectra also accounts for this discrepancy. The inequivalence of the nitrogen isotopes in the $^{14}\text{N}^{15}\text{N}$ molecule introduces a small permanent dipole moment, but the changes in the interactions with the surrounding molecules are expected to be very small. The T_2 time does not depend on the $^{15}\text{N}_2$ concentration and was seen to be but slightly temperature dependent, resulting in a decay time of (118 ± 20) ps for the decay at 30 K.

It should be noted that inhomogeneous broadening, with a width Δ comparable to that observed for the $^{14}\text{N}_2$ vibrons in pure crystals, would not be observable in the relatively fast $^{15}\text{N}_2$ vibrational dephasing. The inhomogeneous contribution to the decay increased for increasing concentrations of $^{15}\text{N}_2$, resulting in an almost completely Gaussian decay for a $^{15}\text{N}_2$ concentration of 8.6 mol% [see Fig. 4(b) and Table I]. In the latter decay spectra, hardly any exponential decay could be resolved. Due to the slightly smaller vibrational frequency and the resulting smaller vibrational amplitude of the heavier isotope, a relative difference in molar volume³

TABLE I. The inhomogeneous (Gaussian) contribution to the linewidth of the $^{14}\text{N}_2$ and $^{15}\text{N}_2$ vibrations, as obtained by fitting the dephasing of $^{14}\text{N}_2$ vibrons and $^{15}\text{N}_2$ vibrations for a varying concentration of $^{15}\text{N}_2$. All decays were recorded at 10 K.

Concentration $^{15}\text{N}_2$ (mol %)	Gaussian FWHM (cm^{-1})	
	$^{14}\text{N}_2$	$^{15}\text{N}_2$
0.0	0.01 ^a	
1.7	(0.018 ± 0.004)	< 0.05
4.7	(0.029 ± 0.005)	
5.4	(0.030 ± 0.007)	(0.16 ± 0.04)
7.8	(0.034 ± 0.007)	(0.19 ± 0.06)
8.6	(0.040 ± 0.009)	(0.20 ± 0.05)

^a Depending on the specific interaction volume in the crystal and the crystal growth procedure.

$[V(^{14}\text{N}_2) - V(^{15}\text{N}_2)]/V(^{14}\text{N}_2) = 0.74\%$ occurs. Different configurations of neighboring $^{15}\text{N}_2$ in the crystal environment cause the inhomogeneous broadening of the Raman transition.

For the relaxation of the $^{14}\text{N}_2$ molecules in mixed crystals of $^{14}\text{N}_2$ with $^{15}\text{N}_2$, no changes in the exponential decay time, T_2 , were resolved. In the same way as observed for the $^{15}\text{N}_2$ decay, an increasing contribution of the Gaussian factor is observed for an increasing concentration of $^{15}\text{N}_2$ [see Fig. 4(a)]. The values of the Gaussian parameter Δ for a series of $^{15}\text{N}_2$ concentrations are listed in Table I. The width increases linearly to almost its quadruple to yield 0.040 cm^{-1} for a $^{15}\text{N}_2$ concentration of 8.6 mol%. It is clear from Table I that the absolute value of the Gaussian parameter, Δ , for the $^{15}\text{N}_2$ stretching vibration is about five times that for $^{14}\text{N}_2$ vibrons. The reduction in inhomogeneous broadening is caused by the vibron coupling of the $^{14}\text{N}_2$ molecules.⁷

A decrease of the factor group splitting of 3% was noticed for the highest concentration of $^{15}\text{N}_2$. The $^{14}\text{N}_2$ molecules possess on the average a smaller number of nearest-neighbor $^{14}\text{N}_2$ with which to couple in the formation of the vibronic excitation. Hereby the overall strength of the vibration-vibration coupling between different sites is reduced.

IV. DISCUSSION AND CONCLUSIONS

The mean-square value σ for the site-energy perturbation can be determined from the inhomogeneous broadening of $^{15}\text{N}_2$ vibrational transition for mixed crystals with low concentrations of $^{15}\text{N}_2$. At low concentrations of $^{15}\text{N}_2$ almost no inhomogeneous broadening is observed, providing an upper limit for σ . The lower limit is determined by the value obtained for the $^{14}\text{N}_2$ vibrons. The width of the Gaussian distribution of site energies, σ , due to crystal disorder should therefore be within the range from 0.01 to 0.05 cm^{-1} , which is again smaller than the values obtained for the polycrystalline samples^{9,11} and than the value obtained in Ref. 9.

The decay time of the $^{15}\text{N}_2$ molecules in the α - $(^{15}\text{N}_2)_x(^{14}\text{N}_2)_{1-x}$ crystals is much smaller than one would expect since the vibrational frequency of $^{15}\text{N}_2$ is about 78 cm^{-1} below that of $^{14}\text{N}_2$. The dephasing time for the isotopic vibrations is expected to be long, since the energy difference between $^{15}\text{N}_2$ and $^{14}\text{N}_2$ or $^{14}\text{N}^{15}\text{N}$ molecules is much too high to be overcome by thermal processes (kT). The $^{15}\text{N}_2$ -doped molecules in the $^{14}\text{N}_2$ crystals were expected to act as traps for the vibrons: Together with the localization of the excitation on the impurity, one or more low-frequency excitations could be created to make up for the 78 cm^{-1} energy difference. However, no reduction of the $^{14}\text{N}_2$ decay time T_2 was found even for a large concentration of $^{15}\text{N}_2$ molecules in the α - $(^{15}\text{N}_2)_x(^{14}\text{N}_2)_{1-x}$ crystal, indicating that this trapping process is not likely to occur. Also, quasielastic scattering of the vibrons by the impurities does not show up

in the measurements. This behavior is very different from the results of recent ps relaxation measurements^{18,19} on rotons in para-H₂ crystals, doped with ortho-H₂ and HD impurities. In these cases, the decay signals could be described by means of a single exponential relaxation time T_2 and no Gaussian factor. The relaxation rate T_2^{-1} was seen to increase linearly with the impurity concentration by about a factor of 5 for a HD or ortho-H₂ concentration of 5 at.%. A possible explanation for the smaller cross-section for scattering lies in the different strength and range of the interactions which are at the origin of the roton (electric quadrupole-quadrupole) and vibron²⁰ formation.

We will now discuss several processes which may be responsible for the observed exponential part of the vibrational decay (T_2) of the $^{14}\text{N}_2$ and $^{15}\text{N}_2$ molecules. Since the vibrational frequency of N₂ is many times larger than the highest phonon and libron frequencies, depopulation of the vibrational excited state (T_1 processes) by phonon emission is a high-order process of negligible contribution. Dephasing due to strains and defects in the crystals appears only as the inhomogeneous component in the observed decay and is not expected to be temperature dependent. Anyhow, no correlation between the T_2 dephasing time and the magnitude of the inhomogeneous contributions in the crystal or the crystal growth technique could be established. Therefore, the observed exponential decay time $T_2/2$ is not caused by dephasing due to strains and defects. The largest concentration of impurities in the $^{14}\text{N}_2$ crystal (grown from 99.9999% pure gas, research grade) comes from the isotopic molecules $^{14}\text{N}^{15}\text{N}$ (0.74 mol%) and $^{15}\text{N}_2$ (0.00014 mol%). Since no reduction of the $T_2/2$ time was observed for a concentration of $^{15}\text{N}_2$ admixture of 8.6 mol%, such small concentrations of impurities are not expected to cause the observed decay. Impurity scattering can thus be eliminated as a possible dephasing mechanism.

We relate the decay, in fact by elimination, to scattering by librations and phonons. For the studied temperature, only low-frequency phonons and zero-point motions of the librations have to be taken into account. Nevertheless, their contribution may be considerable, for the librations in α -N₂ (Ref. 21) are known to behave as very anharmonic oscillators, as was evidenced in nuclear-quadrupole-resonance (NQR) measurements.²² The strong temperature dependence of the NQR resonance frequencies could only be explained by assuming large-amplitude molecular librations with an anharmonic character²² which are present even at the lowest temperatures. The librational frequencies were reproduced by *ab initio* calculations,²³ starting from orientational states, intermediate between harmonic librations and free rotations. Spontaneous Raman measurements in the lattice vibration region²⁴ have shown a gradual removal of orientational ordering towards the α - β phase transition, probably due to the large-amplitude librational motion of the molecules.

While at low temperature the T_2 time of the $^{14}\text{N}_2$ vi-

brons is much longer compared to the $^{15}\text{N}_2$ vibration, they converge to the same value of $T_2/2 \approx 115$ ps at the α - β phase transition. It seems that near this phase transition the $^{14}\text{N}_2$ vibrations are decoupled from site to site and behave like single-molecule excitations, or, in an alternative picture, the interactions with phonons and/or librations strongly reduce the size of the vibrational exciton.

Further information about the observed dephasing process may be gained by studying the relaxation of N_2 molecules as substitutional impurities in rare gas solids,

thereby eliminating the interactions with librational degrees of freedom.

ACKNOWLEDGMENTS

Financial support for two of the authors (J.D.K. and E.G.) from the National Fund for Scientific Research Belgium (NFWO) is gratefully acknowledged. This work was made possible by further financial support from the Inter-University Institute for Nuclear Sciences (IIKW).

-
- ¹S. Velsko and R.M. Hochstrasser, *J. Phys. Chem.* **89**, 2240 (1985).
²A. Penzkofer, A. Laubereau, and W. Kaiser, *Prog. Quantum Electron.* **6**, 55 (1979).
³T.A. Scott, *Phys. Rep.* **27**, 89 (1976).
⁴G.W. Robinson, *Annu. Rev. Phys. Chem.* **21**, 429 (1970).
⁵A. Laubereau and W. Kaiser, *Rev. Mod. Phys.* **50**, 607 (1978).
⁶S.R.J. Breuck and R.M. Osgood, *Chem. Phys. Lett.* **39**, 568 (1976).
⁷J. Klafter and J. Jortner, *J. Chem. Phys.* **68**, 1513 (1978).
⁸I.I. Abram and R.M. Hochstrasser, *J. Chem. Phys.* **72**, 3617 (1980).
⁹I.I. Abram, R.M. Hochstrasser, J.E. Kohl, M.G. Semack, and D. White, *J. Chem. Phys.* **71**, 153 (1979).
¹⁰J. De Kinder, E. Goovaerts, A. Bouwen, and D. Schoemaker, *J. Lumin.* **45**, 423 (1990).
¹¹R. Beck and J.W. Nibler, *Chem. Phys. Lett.* **159**, 79 (1989).
¹²J.D. Kafka and T.M. Baer, *IEEE J. Quantum Electron.* **24**, 341 (1988).
¹³D.D. Dlott, *Annu. Rev. Phys. Chem.* **37**, 157 (1986).
¹⁴T.J. Koscic, R.E. Cline, Jr., and D.D. Dlott, *J. Chem. Phys.* **81**, 4932 (1984).
¹⁵J.W. Nibler and R. Beck (private communication).
¹⁶R.D. Beck, M.F. Hineman, and J.W. Nibler, *J. Chem. Phys.* (to be published).
¹⁷S. Velsko, J. Trout, and R.M. Hochstrasser, *J. Chem. Phys.* **79**, 2114 (1983).
¹⁸C. Sierens, A. Bouwen, E. Goovaerts, M. De Mazière, and D. Schoemaker, *Phys. Rev. A* **37**, 4769 (1988).
¹⁹M. Leblans, A. Bouwen, C. Sierens, W. Joosen, E. Goovaerts, and D. Schoemaker, *Phys. Rev. B* **40**, 6674 (1989).
²⁰G. Zumofen, K. Dressler, M.M. Thiéry, and V. Chandrasekharan, *J. Chem. Phys.* **67**, 5983 (1977).
²¹S. Califano and V. Schettino, *Int. Rev. Phys. Chem.* **7**, 19 (1988).
²²J.R. Brookeman, M.M. McEnnan, and T.A. Scott, *Phys. Rev. B* **4**, 3661 (1971).
²³A.P.J. Jansen, W.J. Briels, and A. Van der Avoird, *J. Chem. Phys.* **81**, 3648 (1984).
²⁴G. Pangilinan, G. Guelachvili, R. Sooryakumar, K.N. Rao, and R.H. Tipping, *Phys. Rev. B* **39**, 2522 (1989).